one arrives at

$$\Delta c_p = (2/\rho_\infty U_\infty^2)(\rho V)^s \cdot V^D = 0 \tag{13}$$

So far, no distinction has been made between subsonic and supersonic speed regimes. Beginning with the next section, the discussion is restricted to the subsonic flow domain.

Application of the Goethert Rule

The boundary conditions of incompressible free vortex flow, which correspond to boundary conditions (7) and (13) of the compressible domain, read

$$V_i^s \cdot n_i = 0 \tag{14}$$

$$\Delta c_{p_i} = (2/U_\infty^2) V_i^s \cdot V_i^D = 0 \tag{15}$$

The subscript i denotes quantities in the incompressible flow domain.

The question now arises as to which, if any, of the various transformations that reduce the compressible potential Eq. (1) to Laplace's equation also reduce the boundary conditions of the compressible domain as given by Eqs. (7) and (13) to their equivalent form in the incompressible flow domain. It can be verified easily that the desired transformation is achieved by application of the following well-known version of the Goethert rule:

$$x_i = x/\beta,\ y_i = y,\ z_i = z,\ \phi_i = \beta\phi,\ \beta = \sqrt{1-M_\infty^2} \tag{16}$$

The freestream velocity is kept fixed during the transformation, but the angle of attack changes as $\tan\alpha_i = \beta \tan\alpha$. By application of the Goethert rule to Eq. (5), one can show further that the pressure distributions of both flow domains are related by

$$c_p = c_{p_i}/\beta^2 \tag{17}$$

where c_{p_i} is obtained from Bernoulli's equation.

It should be emphasized that boundary conditions (14) and (15) of the incompressible flow domain are applied on the surface $z_i = f_i(x_i, y_i)$, and that boundary conditions (7) and (13) of the compressible domain are applied on the surface $z = f(x,y)$, where

$$f_i(x_i, y_i) = f(\beta x_i, y_i) \tag{18}$$

Numerical Results

The accuracy of the Goethert rule used in combination with exact boundary conditions involving the mass flux vector was investigated numerically by calculating the subsonic flow about planar wing geometries over a wide range of angles of attack. The wing planforms were transformed according to Eq. (16), and the resulting incompressible flow problems were solved using a modified version of the numerical technique of Ref. 3. The computed compressible values of lift coefficient c_L, drag coefficient c_D, and pitching moment coefficient c_m are compared in Figs. 1 and 2 with experimental data of Ref. 5. The coefficients are referred to wing area, freestream dynamic pressure, and mean aerodynamic chord. The pitching moment reference axes of the delta wing and the arrow wing are located at 50% and 64.5% root chord, respectively. It is shown in Fig. 1 that the characteristics of the delta wing are very well predicted even at the extreme flight condition of 9 deg angle of attack and 0.8 freestream Mach number. Drag and pitching moment characteristics of the arrow wing are shown in Fig. 2 to be well predicted up to 20 deg angle of attack, although the lift is overpredicted at higher incidences. For comparison, theoretical data of the lift coefficient obtained from the leading-edge suction analogy of Polhamus[2] also are shown; the agreement with the theoretical results of the method reported in this Note is remarkable.

Acknowledgment

This research was supported partly by NASA Langley under Contract NAS1-13833 and partly by the Independent Research and Development Program of The Boeing Company. The authors wish to thank Forrester T. Johnson and Paul Lu of The Boeing Company for their support in generating some of the numerical results.

References

[1] Kandil, O. A., Mook, D. T., and Nayfeh, A. H., "Effect of Compressibility on the Nonlinear Prediction of the Aerodynamic Loads on Lifting Surfaces," AIAA Paper 75-121, Pasadena, Calif., Jan. 20-22, 1975.

[2] Polhamus, E. C., "Charts for Predicting the Subsonic Vortex-Lift Characteristics of Arrow, Delta, and Diamond Wings," NASA TN D-6243, 1971.

[3] Weber, J. A., Brune, G. W., Johnson, F. T., Lu, P., and Rubbert, P. E., "A Three-Dimensional Solution of Flows Over Wings with Leading Edge Vortex Separation," *AIAA Journal*, Vol. 14, April 1976, pp. 519-525.

[4] Ward, G. N., *Linearized Theory of Steady High-Speed Flight*, Cambridge University Press, London, 1955.

[5] Davenport, E. E., "Aerodynamic Characteristics of Three Slender Sharp-Edge 74° Swept Wings at Subsonic, Transonic, and Supersonic Mach Numbers," NASA TN D-7631, 1974.

Centroidal and Area Average Resistances of Nonsymmetric, Singly Connected Contacts

M. M. Yovanovich* and S. S. Burde†
University of Waterloo, Waterloo, Ontario, Canada

Introduction

IT was demonstrated in a recent paper[1] that the normalized constriction resistance $\lambda\delta R$ is approximately equal to the value 5/9 and 84% of this value when δ is chosen to be the square root of the contact area and when the resistance in the first instance is based upon the centroid temperature and in the second upon the area average temperature. This remarkable fact was observed for a set of singly connected, symmetric planar contacts of the form $(x/a)^n + (y/b)^n = 1$, with $b = a$ subject to the same uniform heat flux. The geometric parameter n was allowed to range from $n = \frac{1}{2}$ to $n = \infty$, thereby covering a variety of shapes which included astroids, a circle, a square, and near squares.

To determine whether the results of the symmetric study are general, three nonsymmetric shapes were examined. This Note describes the method used to obtain the temperature at arbitrary points and the centroidal temperature for a triangular contact, a semicircular contact, and an L-shaped contact. A numerical method was used to obtain the area average temperature of these contact areas.

Arbitrary and Area Average Temperatures

Triangular Contact Area

Figure 1 shows a singly connected, planar triangular contact area of base $2a$ and height $2b$ subjected to a uniform heat flux q. The half-space thermal conductivity is λ. The expression for the normalized resistance based upon the area

Received April 1, 1977; revision received July 11, 1977.
Index categories: Spacecraft Temperature Control; Heat Conduction; Thermal Modeling and Analysis.

*Professor, Thermal Engineering Group, Department of Mechanical Engineering. Associate Fellow AIAA.
†Graduate Research Assistant, Thermal Engineering Group, Department of Mechanical Engineering.

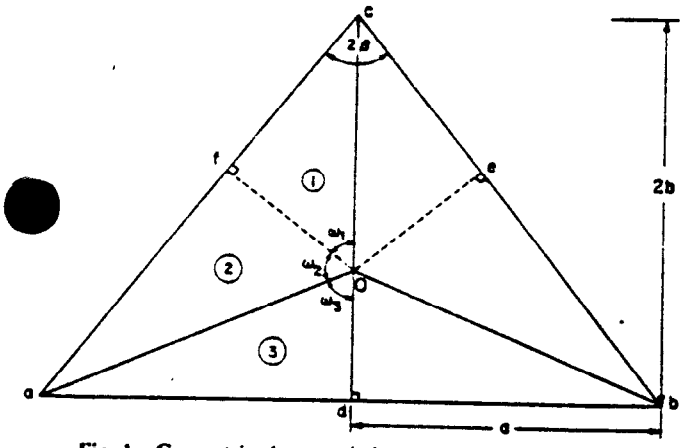

Fig. 1 Geometric characteristics of the triangular contact.

average temperature and the square root of the area was obtained and evaluated numerically by the procedure described in Ref. 1 for various values of the aspect ratio $\alpha(=b/a)$. It was found that the average value of $\lambda\sqrt{A}\,\bar{R}=0.4525$ in the range $0.4\le\alpha\le 2$. The largest and the smallest differences in the values were $+1.75\%$ and -2.36% for $\alpha=0.8$ and 2, respectively. The resistance changed considerably from the average value for $\alpha<0.4$ and $\alpha>2$.

Figure 1 is used to obtain an exact analytical expression for the centroidal temperature. The lines joining the centroid (located a distance $2b/3$ from the base) to the three vertices and the three perpendiculars from the centroid to the three sides form three pairs of identical right triangles.

From the geometry, we obtain the relationship

$$\beta=\tan^{-1}(1/2\alpha) \tag{1}$$

where $\alpha=(cd)/(2ad)$. The three angles subtended at the centroid can be obtained as follows:

$$\omega_1=(\pi/2)-\beta,\quad \omega_3=\tan^{-1}(3\tan\beta) \tag{2a}$$

$$\omega_2=\pi-\omega_1-\omega_3 \tag{2b}$$

Adding the effects of the six triangles, we obtain the following expression for the centroidal temperature:

$$\frac{\pi\lambda}{q}T_0=\tfrac{1}{3}\sin 2\beta\,\ell_n\left[\tan\left(\frac{\pi}{4}+\frac{\omega_1}{2}\right)\tan\left(\frac{\pi}{4}+\frac{\omega_2}{2}\right)\right]$$

$$+\tfrac{1}{3}\cos\beta\,\ell_n\tan\left(\frac{\pi}{4}+\frac{\omega_3}{2}\right) \tag{3}$$

where

$$od=\tfrac{1}{3}\cos\beta,\qquad oe=of=\tfrac{1}{3}\sin 2\beta \tag{4}$$

The normalized constriction resistance based upon the centroidal temperature and the square root of the contact area is

$$\lambda\sqrt{A}\,R_0=(\lambda T_0/q)\sqrt{2/\sin 2\beta} \tag{5}$$

with $(\lambda T_0/q)$ obtained from Eq. (3).

For $0.4\le\alpha\le 2$, it was observed that the average value of $\lambda\sqrt{A}R_0=0.5421$, and the largest and the smallest differences in values were $+1.75\%$ and -2.71% for $\alpha=1$ and 2, respectively. For $\alpha<0.4$ and $\alpha>2$, the difference from the average value was considerable. In the same range of α, the average value of $\bar{R}/R_0$ was 0.8348, and the difference from the average value was insignificant even for a larger range of α.

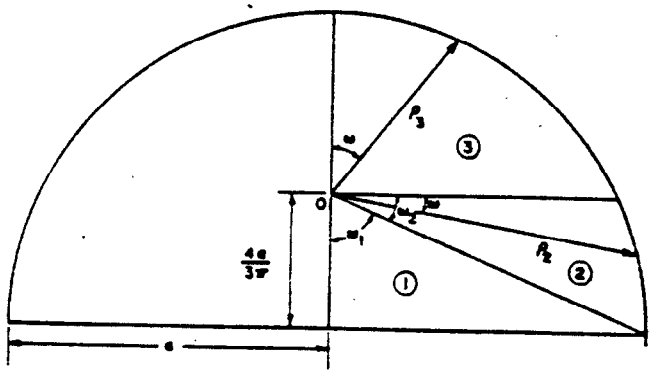

Fig. 2 Geometric characteristics of the semicircular contact.

Semicircular Contact

The second nonsymmetric contact area studied is shown in Fig. 2. The local and area average temperatures for the semicircular contact of radius a are obtained using the procedure discussed in Ref. 1. It is found that $\lambda\sqrt{A}\bar{R}=0.4610$ for this contact area.

To determine the centroidal temperature, we take advantage of symmetry about the vertical axis and divide one-half of the contact area into the three areas shown in Fig. 2. The apex of the right triangle is placed at the centroid, which is a distance $(4a/3\pi)$ from the base. The angle ω_1 at the apex is known to be

$$\omega_1=\tan^{-1}(3\pi/4) \tag{6}$$

and, since $\omega_3=\pi/2$, we can determine ω_2. The contribution of the triangular area to the centroidal temperature follows directly[2]:

$$T_1=\frac{q}{2\pi\lambda}\frac{4a}{3\pi}\ell_n\tan\left(\frac{\pi}{4}+\frac{\omega_1}{2}\right) \tag{7}$$

The contribution of area 2 to the centroidal temperature can be obtained by means of the following expressions[2]:

$$T_2=\frac{q}{2\pi\lambda}\int_0^{\omega_2}\rho_2\,d\omega \tag{8}$$

where, from Fig. 2, we have

$$\rho_2=a[\upsilon\sin\omega+\sqrt{1-\upsilon^2\cos^2\omega}] \tag{9}$$

with $\upsilon=4/3\pi$. After substitution of Eq. (9) into Eq. (8), we have, according to Ref. 3,

$$T_2=\frac{qa}{2\pi\lambda}\left[\upsilon(1-\cos\omega_2)+E\left(\sin^{-1}\frac{\sin\omega_2}{(1-\upsilon^2\cos^2\omega_2)^{1/2}},\upsilon\right)\right.$$

$$\left.-\frac{\upsilon^2\sin\omega_2\cos\omega_2}{(1-\upsilon^2\cos^2\omega_2)^{1/2}}\right] \tag{10}$$

Since

$$\sin\omega_2=\frac{\upsilon}{(1+\upsilon^2)^{1/2}},\quad \cos\omega_2=\frac{1}{(1+\upsilon^2)^{1/2}} \tag{11}$$

Eq. (10) can be reduced to the following expression[4]:

$$T_2=(qa/2\pi\lambda)\,[\upsilon-\upsilon(1+\upsilon^2)^{1/2}+E(\sin^{-1}\upsilon,\upsilon)] \tag{12}$$

where E is the incomplete elliptic integral of the second kind of amplitude $\sin^{-1}\upsilon$ and modulus υ.

The contribution of the remaining area of Fig. 2 is obtained by means of Eq. (8) and the radius vector:

$$\rho_3 = a[-v\cos\omega + (1-v^2\sin^2\omega)^{1/2}] \quad (13)$$

Therefore, after substitution of Eq. (13) into Eq. (8) and integration, we have

$$T_3 = (qa/2\pi\lambda)[E(v) - v] \quad (14)$$

where E is the complete elliptic integral of the second kind of modulus v.

Adding Eqs. (7, 12, and 14) and multiplying by 2 yields the centroidal temperature. Dividing this temperature by the total heat flow rate and then normalizing this value yields the dimensionless centroidal resistance:

$$\lambda\sqrt{A}\,R_0 = \frac{1}{\pi}\sqrt{\frac{2}{\pi}}\left[v\ln\tan\left(\frac{\pi}{4}+\frac{1}{2}\tan^{-1}\frac{1}{v}\right)\right.$$
$$\left. + E(\sin^{-1}v, v) + E(v) - v(1+v^2)^{1/2}\right] \quad (15)$$

Since $v = 4/3\pi$, Eq. (15) reduces to $\lambda\sqrt{A}\,R_0 = 0.5456$. The ratio of the area average resistance to the centroidal resistance for this contact area is 0.8449.

L-Shaped Contacts

The desired L-shaped contact is generated by the removal of a rectangular area ($\xi\eta$) from the lower left-hand corner of a unit square area. The origin of the Cartesian coordinate system is located at the lower left-hand corner of the unit square. The centroidal and area average temperatures and the corresponding dimensionless resistances were obtained by varying ξ and η systematically. In this work, ξ was allowed to range from 0 to 0.5 with increments of 0.10, while η ran from 0 to 1.0 for each value of ξ, in increments of 0.10. In this manner, 50 different L-shaped contacts were examined.[4]

When $\xi = \eta = 0.1$, the largest values of the dimensionless resistances were observed, these being $\lambda\sqrt{A}\,\bar{R} = 0.4733$ and $\lambda\sqrt{A}\,R_0 = 0.5614$. The smallest values, $\lambda\sqrt{A}\,\bar{R} = 0.4424$ and $\lambda\sqrt{A}\,R_0 = 0.5197$ were observed at $\xi = 0.5$, $\eta = 0.7$. The maximum value of $\bar{R}/R_0 = 0.8540$ occurred at $\xi = 0.5$, $\eta = 0.6$, while the minimum value of $\bar{R}/R_0 = 0.8321$ was noted at $\xi = 0.5$, $\eta = 0.9$. They differ from the value of 0.8400 by +1.67% and −0.95%, respectively.

Summary and Conclusion

We see that, in the range $0.4 \le \alpha \le 2$, both constriction resistances, $\bar{R}$ and R_0, are relatively insensitive to the aspect ratio and, further, that these triangular shapes have constriction resistances that do not differ substantially from the constriction resistances of a circular contact area ($\lambda\sqrt{A}\bar{R} = 0.4787$, $\lambda\sqrt{A}R_0 = 0.5642$). For $\alpha < 0.4$ and $\alpha > 2$, both resistances decrease, and these values no longer can be considered comparable to those of the circular contact area. We note that the ratio $\bar{R}/R_0$ is much less sensitive to the aspect ratio α over its entire range, and that the values agree closely with the ratio corresponding to the circular contact. The results of the analysis for the semicircular contact area are remarkable for two reasons:

1) The normalized resistances are less than 4% different.

2) These resistances are less than the corresponding resistances for the circular contact; that is to say, the nonsymmetric contact offers less constriction resistance than the symmetric contact area.

The L-shaped contact area results are even more remarkable because, although this contact has no symmetry, its constriction resistance is very close to that of the triangular and semicircular contact areas and smaller than that of the circular contact. Its ratio $\bar{R}/R_0$ is in remarkably good agreement with the results of the triangular and semicircular contact areas.

The results of this study allow us to conclude that one can estimate the area average temperature (or constriction resistance) of nonsymmetric contact areas by taking 84% of the centroidal temperature (or constriction resistance) with an error less than ±1.7%, provided that the contact area is not too asymmetric. The constriction resistance of nonsymmetric contact areas, whether based upon the area average or centroidal temperatures, will be less than the corresponding resistances for the circular contact. The normalized constriction resistance $\lambda\sqrt{A}\,R_0$ is approximately 5/9 for symmetric and nonsymmetric contacts when subjected to a uniform heat flux.

Acknowledgment

The authors thank the National Research Council for its financial support.

References

[1] Yovanovich, M. M., Burde, S. S., and Thompson, J. C., "Thermal Constriction Resistance of Arbitrary Planar Contact with Constant Flux," AIAA *Progress in Astronautics and Aeronautics: Thermophysics of Spacecraft and Outer Planet Entry Probes*, Vol. 56, edited by A. M. Smith, New York, 1977, pp. 127-140.

[2] Yovanovich, M. M., "Thermal Constriction Resistance of Contacts on a Half-Space: Integral Formulation," AIAA *Progress in Astronautics and Aeronautics: Radiative Transfer and Thermal Control*, Vol. 49, edited by A. M. Smith, New York, 1976, pp. 397-418.

[3] Gradshteyn, I. S. and Ryzhik, I. M., *Table of Integrals, Series, and Products*, Academic Press, New York, 1965.

[4] Burde, S. S., "Thermal Contact Resistance between Smooth Spheres and Rough Flats," Ph.D. Thesis, Dept. of Mechanical Engineering, Univ. of Waterloo, Ontario, March 1977.

Determination of Pole Sensitivities by Danilevskii's Method

James B. Nail,* Jerrel R. Mitchell,† and Willie L. McDaniel Jr.‡
Mississippi State University, Mississippi State, Miss.

I. Introduction

IN control theory, a synonymous term to pole sensitivity is eigenvalue sensitivity. Several methods for calculating eigenvalue sensitivities have been presented.[1-5] In general, these methods either require an application of Leverrier's method[2] or require the determination of eigenrows and eigencolumns.[1,3-5] Although Leverrier's method has a theoretically sound basis, it suffers from truncation errors when implemented on a digital computer. From experience these authors have found that numerical results from Leverrier's method cannot be trusted for systems roughly greater than tenth order.§

The techniques utilizing eigenrows and eigencolumns are suitable if the sensitivities of only a few eigenvalues are sought. However, if the sensitivities of several eigenvalues are required, then the calculation of the needed eigenrows and eigencolumns can be a formidable task.

In this paper, an alternate approach for calculating sensitivities of poles and eigenvalues is presented. Danilevskii's

Received April 18, 1977; revision received June 9, 1977.
Index category: Analytical and Numerical Methods.
*Research Associate, Department of Aerospace Engineering.
†Associate Professor, Department of Electrical Engineering.
‡Professor, Department of Electrical Engineering.
§This conclusion was reached while using a UNIVAC 1106 with